Journal of
Marine Science and Engineering

MDPI

Article

Optimization of Energy Consumption in Ship Propulsion Control under Severe Sea Conditions

Zhiyuan Yang [1], Wendong Qu [1,*] and Jianyu Zhuo [2]

[1] Merchant Marine College, Shanghai Maritime University, Shanghai 201306, China; yangzy@shmtu.edu.cn
[2] China Classification Society, Beijing 100008, China; jyzhuo@ccs.org.cn
* Correspondence: 202230110106@stu.shmtu.edu.cn

Abstract: With the further establishment of relevant regulations on ship emissions by countries worldwide and the IMO, and the increasing frequency of severe sea conditions in shipping routes, optimizing ship energy efficiency under high wind and wave conditions has become an important research direction. This study establishes a grey-box model for optimizing ships' energy consumption under severe sea conditions, with wave heights above two meters and a Beaufort scale score above five, based on the principle of ship–engine–propeller matching and a non-dominated sorting optimization algorithm. Using historical navigation data from a case ship under severe sea conditions, a white-box model and a black-box model for ship fuel consumption were established. These models were combined to create a grey-box model for ship fuel consumption. The K-Medoids clustering algorithm was used to cluster severe sea conditions. The optimization variables were the main engine's speed, with the fuel consumption per nautical mile and the ship's speed being used as optimization objectives. The non-dominated sorting genetic algorithm was optimized for each sea condition, resulting in the best speed for each sea state. The results indicate that the model developed in this paper reduced the main engine's fuel consumption per nautical mile by 21.9% and increased the speed by 16.7% under the most severe sea conditions. Therefore, the proposed model effectively optimizes ship energy efficiency and reduces navigation time under severe sea conditions, providing an effective solution for operations in actual severe sea conditions.

Keywords: rough sea; fuel consumption optimization; grey-box model

Citation: Yang, Z.; Qu, W.; Zhuo, J. Optimization of Energy Consumption in Ship Propulsion Control under Severe Sea Conditions. *J. Mar. Sci. Eng.* **2024**, *12*, 1461. https://doi.org/10.3390/jmse12091461

Received: 17 July 2024
Revised: 5 August 2024
Accepted: 21 August 2024
Published: 23 August 2024

1. Introduction

The shipping industry makes a significant contribution to global trade, with over 80% of goods being transported by sea annually. Although carbon emissions from shipping constitute only a small portion of global carbon emissions, the share of shipping emissions in global anthropogenic emissions increased from 2.76% in 2012 to 2.89% in 2018 [1]. According to the United Nations Conference on Trade and Development's (UNCTAD) "Review of Maritime Transport 2023," this proportion has further risen to 3% [2]. In response, the International Maritime Organization (IMO) set forth short-term and long-term decarbonization targets in 2023: a 40% reduction in carbon intensity by 2030 and near-zero emissions by around 2050 [3]. The short-term targets include measures such as the Energy Efficiency Existing Ship Index (EEXI), Carbon Intensity Indicator (CII), and Ship Energy Efficiency Management Plan (SEEMP) [4]. At the same time, as the global economy enters a downturn and the shipping market continues to decline with decreasing freight rates, fuel costs account for more than 50% of the daily operational costs of ships [5]. Currently, emission reduction measures for existing operational ships primarily include ship intelligence, the application of energy-saving devices, route optimization, and speed optimization. Among these, speed optimization [6] has a particularly significant impact on energy savings and emission reductions for existing ships, simultaneously lowering operational costs and addressing the increasingly stringent emission targets set by the IMO.

In recent years, many scholars have conducted studies on ship speed reduction. Degiuli [7] studied speed reduction in Panamax container ships in specific areas of the Mediterranean Sea, and the author indicated that a 13.6% reduction in speed could save up to 31% of fuel consumption and greenhouse gas emissions in all surveyed areas. Farkas et al. [8] conducted studies on Panamax container ships on fixed routes, analyzing speed reductions of 10% to 40% annually and monthly. They found that an annual speed reduction of 40% could reduce fuel consumption per nautical mile by up to 29.2% on the North Atlantic route.

Currently, there are three main types of ship fuel consumption models: white-box models, black-box models, and grey-box models [9]. The white-box model is based on the principles of ship propulsion. Tillig et al. [10] established a white-box model for the main engine's fuel consumption based on the principle of ship–engine–propeller matching. This model is very intuitive, allowing a direct functional relationship between the main engine's fuel consumption and the ship's speed [11]. Researchers use the principle of ship–engine–propeller matching to build a white-box model using simulation platforms. Tran et al. [12] developed a ship energy consumption model directly using the SIMULINK R2023a platform. However, in actual ship operations, the sea conditions are very complex, and the white-box model often cannot adequately reflect the impact of the external environment on the main engine. Therefore, the accuracy of the white-box model is less ideal under high wind and wave conditions [13]. The black-box model is a purely data-driven fuel consumption model, mainly divided into statistical models and machine learning models [14]. Unlike the white-box model, which is entirely based on physical principles, the black-box model cannot directly show the functional relationship between fuel consumption and ship speed. Ma et al. [15] used the main engine's speed as the optimization variable, optimizing for fuel consumption and sailing time. They employed the K-means clustering algorithm to classify sea conditions based on wind speed, wind direction, and current speed and used the multi-objective particle swarm optimization (MOPSO) algorithm to optimize fuel consumption across different segments. Due to the lack of a clear functional relationship, the accuracy of the black-box model is highly dependent on the settings of model parameters, which significantly affect the results [16].

The grey-box model combines physical principles with data analysis [17], offering the advantages of both white-box and black-box models. Grey-box models can be structured in series or parallel configurations. Cai [18] used big data from ships to develop an efficient and reliable fuel consumption prediction model, exploring the impact of data diversity, quality, and quantity on black-box and grey-box models. They demonstrated that grey-box models could achieve higher accuracy with less data compared to black-box models. Ma et al. [19] optimized ship speed and routes using the NSGA2 algorithm, targeting shipping costs and emissions as optimization objectives. These studies demonstrate that it is feasible to optimize ship energy consumption by controlling the main engine's speed through the establishment of grey-box models for ship fuel consumption based on different sea conditions. Current research on ship energy optimization based on ship–engine–propeller matching mostly focuses on overall speed reduction for routes or speed optimization for specific segments. However, the frequency of high wind and wave conditions on major routes is increasing in some cases. For example, during winter, it is nearly impossible to completely avoid high wind and waves when navigating across the Pacific and Atlantic Oceans in mid to high latitudes. Successive cyclones or cyclone groups can cause severe sea conditions spanning thousands of nautical miles, making avoidance impractical. Therefore, this study establishes a ship energy consumption model that considers the increased impact of high wind and wave conditions on fuel consumption by using the main engine's speed as a variable. It provides an operational solution for actual severe sea conditions.

In this study, a white-box model for ship fuel consumption was established on the SIMULINK simulation platform based on the principle of ship–engine–propeller matching. On the MATLAB platform, ship noon reports (including the daily average main engine power, daily average speed, daily average fuel consumption, daily average ship speed,

and 24 h sailing distance), AIS data (including heading, ship speed, and other navigational information), onboard sensor data, weather forecasts, and data from the fifth generation of the ECMWF atmospheric reanalysis dataset (ERA5) [20] were integrated. The K-Medoids clustering algorithm was used to cluster the collected sea condition data. Using the Random Forest Regression (RFR) algorithm, ship fuel consumption and speed were predicted. The non-dominated sorting genetic algorithm II (NSGA-II) [21] was optimized, incorporating variable weighting, discrete optimization, and the ideal point method. For different sea conditions, the weights were adjusted accordingly. Using the main engine's speed as the optimization variable and fuel consumption per nautical mile and ship speed as optimization objectives, a black-box model for the main engine's fuel consumption was established. The black-box model was combined with the white-box model in series to develop a grey-box model for optimizing ship fuel consumption under high wind and wave conditions.

2. Materials and Methods

This study employs a series-structured grey-box model for fuel consumption, consisting mainly of a fuel consumption calculation module and a main engine speed optimization module. The energy optimization process is illustrated in Figure 1. The white-box model calculates the ship's navigation resistance and fuel consumption, while the black-box model predicts speed, RPM, and fuel consumption. The optimized NSGA-II algorithm is then used to optimize RPM. Finally, the optimized RPM, speed, and sea conditions are input into the fuel consumption calculation module to derive the optimized fuel consumption.

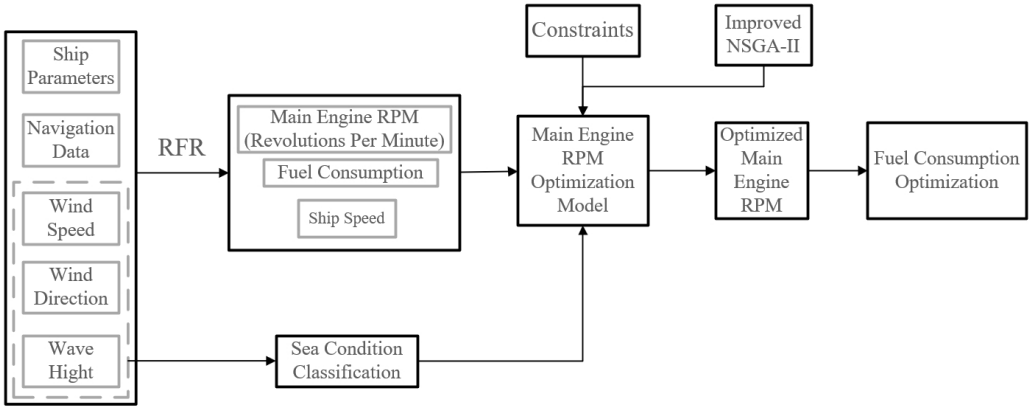

Figure 1. Ship fuel consumption optimization process.

2.1. The Establishment of the White-Box Model

The white-box model is established based on the principle of ship–engine–propeller matching and consists of resistance calculation and fuel consumption calculation modules. The ship's navigation resistance is calculated in three parts: still-water resistance, wave-added resistance, and wind resistance. The still-water resistance is calculated using the classical Holtrop method [22].

In heavy sea conditions, the waves encountered by the bow of the ship include a combination of irregular and regular waves. The added resistance from regular waves is calculated using a semi-empirical formula developed by Liu and Papanikolaou [23]. The second-order transfer function of the added resistance in regular waves can be determined as the sum of the resistance increase due to ship motion and wave reflection. The diffraction component of the wave-induced resistance increase, which dominates in short waves, is calculated based on the pressure integration along the non-shadow region of the waterline, depending on the shape of the waterline relative to the bow and stern and the heading of the incident waves. The radiative component of the added resistance is determined based on the ship's main characteristics, regular wave properties, ship speed, and gyration radius. By analyzing the ship's response to incident waves, the peak positions and the values of the added resistance in the waves can be estimated. The resistance of irregular waves is

calculated using the linear assumption of ship response and the superposition principle of wave and resistance spectra. The additional wave resistance is approximated as the second-order drift force in head waves. The formula for calculating the average added wave resistance is as follows:

$$\Delta\overline{R}_{AW} = 2\int_0^{\infty} \frac{R_{AW}(\omega_e)}{S_a^2} S_\varsigma(\omega_e) d\omega_e \quad (1)$$

In Equation (1), S_ς is the wave frequency, S_a is the significant wave height, and ω_e is the encounter frequency derived from the JONSWAP wave spectrum [24].

$$S_\varsigma(\omega) = \alpha H_S^2 \omega_p^4 \omega^{-5} e^{-\frac{5}{4}\left(\frac{\omega}{\omega_p}\right)^{-4}} \gamma^a \quad (2)$$

where H_s is the significant wave height, ω_p represents the frequency corresponding to the spectral peak, and γ is obtained from the wave spectrum.

Wind resistance is calculated using the ITTC wind resistance coefficients [25]. The formula for calculating the wind resistance of an actual ship is as follows:

$$R_{AA} = 0.5\rho_A C_{AA}\left(\psi_{WRref}\right) A_{AV} V_{WRref}^2 - 0.5\rho_A C_{AA}(0) A_{AV} V_G^2 \quad (3)$$

In Equation (3), ρ_A is the air density; ψ_{WRref} is the relative wind direction at the reference height; V_{WRref} is the relative wind speed at the reference height; A_{AV} is the frontal area; $C_{AA}\left(\psi_{WRref}\right)$ is the wind resistance coefficient at the reference height for a relative wind direction angle of ψ_{WRref}; and V_G is the ground speed.

The specific fuel oil consumption (SFOC) of the main engine depends on the engine model, with significant variations between different engines. It is usually determined through bench tests. This study focuses on a Handymax bulk carrier, whose main engine typically uses heavy fuel oil during daily operations. Using bench test fuel consumption data from the engine manufacturer and actual navigation fuel consumption data from the case ship, a main engine fuel consumption model was established by fitting the engine speed, output power, and fuel consumption, as shown in Figure 2.

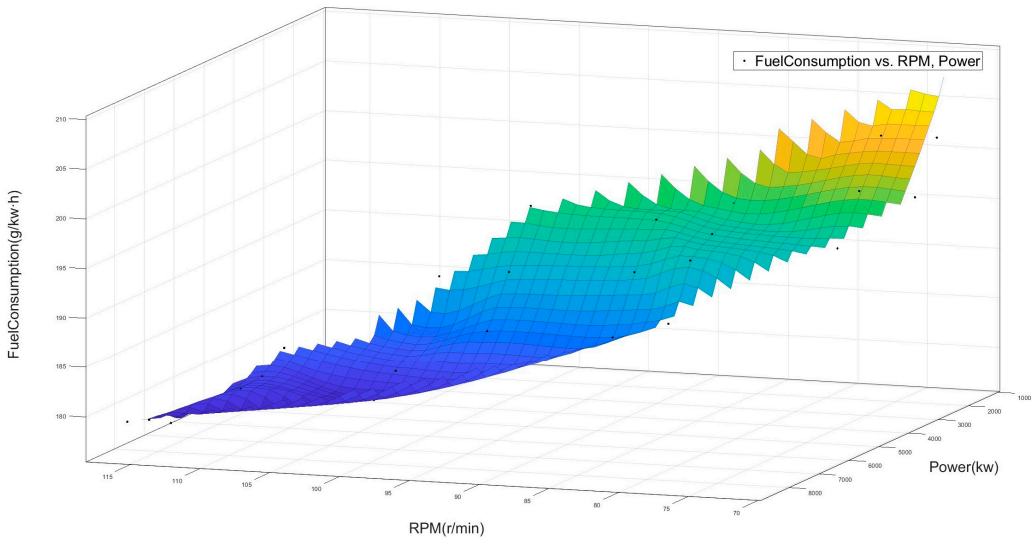

Figure 2. Fitting of RPM, output power, and fuel consumption.

The propeller performance is calculated using the classical regression formula method. The open water efficiency of the propeller is calculated using the following formula:

$$\eta_O = \frac{J}{2\pi}\frac{K_T}{K_Q} \tag{4}$$

In Equation (4), J is the advance coefficient; K_T is the thrust coefficient; and K_Q is the torque coefficient.

2.2. Sea Condition Classification

During navigation, factors affecting the main engine fuel consumption of a ship include the ship's speed, draft, heading, trim, as well as external sea conditions such as wind speed, wind direction, wave height, wave direction, wave period, current speed, and current direction. The Spearman rank correlation coefficient is used to measure the monotonic correlation between two features. As shown in Figure 3, the Spearman rank correlation coefficients between main engine fuel consumption and various factors indicate that the correlation between the ship speed and main engine fuel consumption is the strongest at 0.79. The correlation between draft and main engine fuel consumption is relatively weak, and the influence of heading and trim on main engine fuel consumption is the weakest. For external sea conditions, the correlation coefficients between wind speed, wind direction, wave height, and main engine fuel consumption are the highest, indicating a strong influence of these factors on main engine fuel consumption. Consequently, this study selected sea conditions encountered by the case ship in the past year with an average wave height greater than 2 m and a Beaufort scale score above 5. The K-Medoids algorithm was used for sea condition clustering.

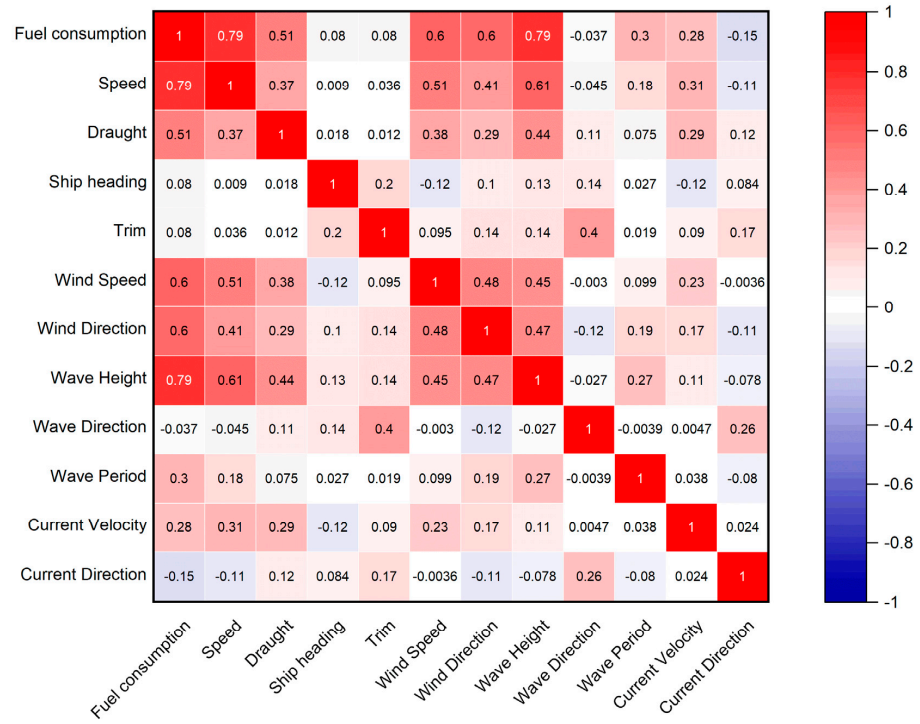

Figure 3. Spearman's rank correlation coefficients for fuel consumption.

The average data of high wind and waves encountered in the past year were selected for sea condition clustering. The sea condition data included wave height, wind speed, and wind direction. By comparing the clustering results under different k values multiple times, the optimal k value was determined to be 6. The clustering results are shown in Figure 4.

The final six cluster centroids represent six typical high wind and wave conditions, as detailed in Table 1. In Table 1, condition 1 represents a relatively severe sea condition with an average wave height of 2.48 m, an average wind speed of 6.92 m/s, and a relative

wind direction of 320°, while condition 6 represents the most severe sea condition with an average wave height of 5.3 m, an average wind speed of 13.67 m/s, and a relative wind direction of 45°. As seen from the data, the severity of the navigational environment varies greatly under different sea conditions. Therefore, by analyzing and reasonably classifying the sea conditions along the route, ship energy consumption management can be conducted more effectively and efficiently in harsh environments.

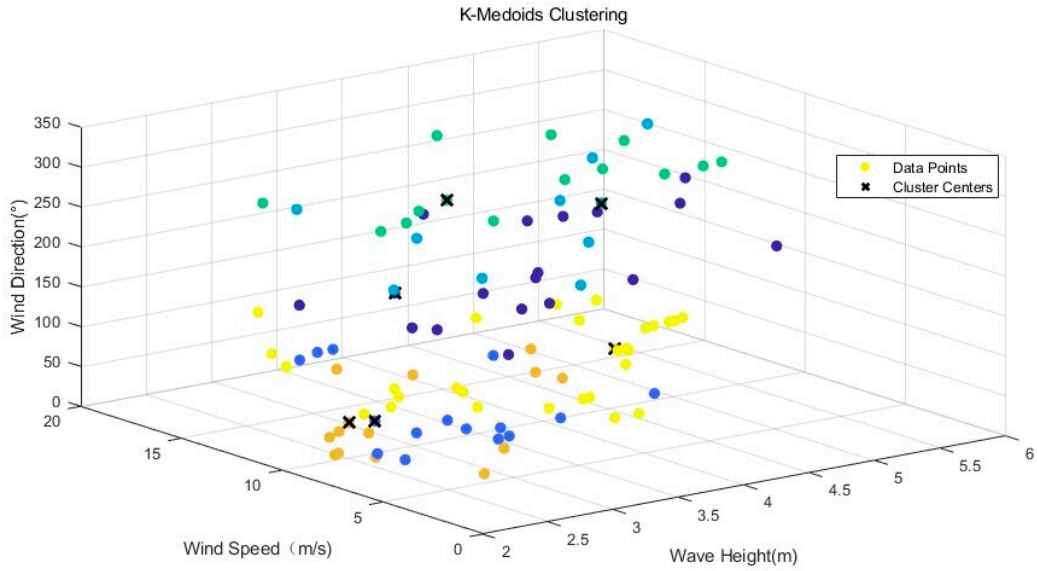

Figure 4. Sea condition clustering results.

Table 1. Sea condition cluster centroids.

Sea Condition	Wave Height (m)	Wind Speed (m/s)	Wind Direction (°)
1	2.48	6.92	320
2	2.74	10.49	20
3	3.47	9.5	180
4	4.00	10.44	90
5	4.44	9.99	40
6	5.30	13.67	45

2.3. The Establishment of the Black-Box Model for Fuel Consumption

In this study, a black-box model was constructed using the Random Forest Regression (RFR) algorithm [26] due to the nonlinear relationship and high dimensionality of the input sea conditions, navigation data, and main engine fuel consumption. The RFR algorithm constructs multiple decision trees and integrates their results, significantly improving the model's prediction accuracy. The structure diagram is shown in Figure 5.

The basic idea is to determine the final output through majority voting among multiple decision trees, thereby reducing the overfitting phenomenon of a single decision tree and providing good anti-overfitting capability. The main steps of the RFR model are as follows:

1. Data sampling: Randomly sample multiple subsets with replacement from the original dataset.
2. Decision tree construction: Build a regression decision tree for each subset. During the construction process, randomly select a subset of features to split nodes.
3. Ensemble results: Average the predictions of all decision trees to obtain the final regression result.

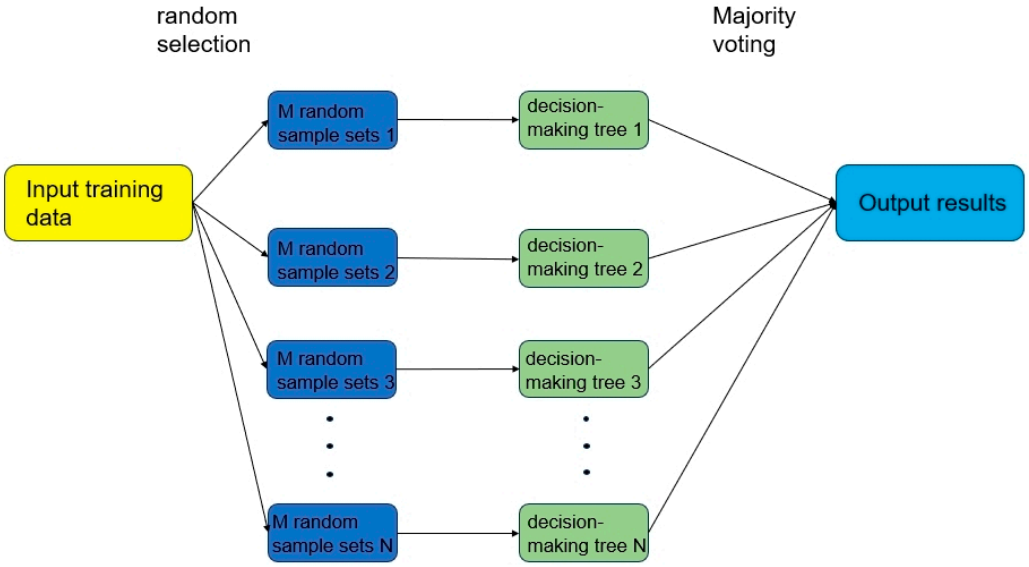

Figure 5. RFR algorithm structure diagram.

The optimal parameters of the model were determined through cross-validation and grid search, as shown in Table 2.

Table 2. Main parameters of RFR.

Parameter Name	Value
N-estimators	200
Max-depth	10
Min-samples-split	5
Min-samples-leaf	2
Max-features	Sqrt
Bootstrap	True
Oob-score	True
N-jobs	1
Random-state	42
Verbose	1

2.4. Validation of the Black-Box Model

This study focuses on a 55,000-ton bulk carrier under full load conditions to establish a dynamic fuel consumption control model under high wind and wave conditions. The main parameters of the study ship are provided in Table 3.

Table 3. Main parameters of the study ship.

Parameter Name	Value
Length Between Perpendiculars (m)	182.65
Waterline Length (m)	189.99
Beam (m)	32.29
Draft (m)	12.48
Displacement (t)	63833
Rated Power (kW)	8208
Rated Speed (r/m)	116
Service Speed (kn)	14.0
Fuel Consumption (t/d)	34

The collected data were divided into two groups; 85% was used for the model training dataset, and 15% for the model validation dataset. To validate the fuel consumption

predictions under six sea conditions, four indicators were introduced as evaluation metrics for model performance: R-squared (R^2) value, Root Mean Squared Error (RMSE), Mean Absolute Error (MAE), and Mean Absolute Percentage Error (MAPE). The predicted results for speed, RPM, and fuel consumption are shown in Tables 4–6. R^2 indicates the degree of agreement between the predicted and actual values, the RMSE is the square root of the sum of squared prediction errors, the MAE is the average of absolute errors, and the MAPE is the relative deviation between predicted and actual values [27].

Table 4. Speed prediction results.

Sea Condition Number	R^2	RMSE	MAE	MAPE
1	0.978	0.078	0.067	0.075%
2	0.976	0.027	0.025	0.030%
3	0.980	0.091	0.079	0.084%
4	0.978	0.148	0.104	0.106%
5	0.981	0.027	0.026	0.023%
6	0.973	0.034	0.026	0.019%

Table 5. RPM prediction results.

Sea Condition Number	R^2	RMSE	MAE	MAPE
1	0.991	0.034	0.031	0.045%
2	0.961	0.055	0.044	0.026%
3	0.974	0.081	0.039	0.049%
4	0.987	0.049	0.042	0.391%
5	0.985	0.032	0.035	0.040%
6	0.978	0.028	0.031	0.048%

Table 6. Fuel consumption prediction results.

Sea Condition Number	R^2	RMSE	MAE	MAPE
1	0.982	0.623	0.071	0.093%
2	0.977	0.255	0.467	0.005%
3	0.963	0.620	0.278	0.012%
4	0.979	0.382	0.308	0.032%
5	0.968	0.921	0.390	0.048%
6	0.965	0.587	0.190	0.075%

In Tables 4–6, it can be seen that the R^2 values of the model predictions are all between 0.96 and 0.99, and the maximum MAPE does not exceed 1%. This indicates that the model established in this study can adapt well to various sea conditions, and its prediction performance and accuracy meet the requirements for subsequent optimization.

2.5. Validation of the Grey-Box Model

The trained white-box model and black-box model were combined in series to establish a grey-box model for optimizing ship energy consumption. By comparing the data in Table 7, it can be seen that the speed predicted by the grey-box model is slightly higher than the actual speed, with a difference between 0.1 and 0.2 knots. In sea conditions 1 to 4, the speed predicted by the grey-box model is slightly higher than the actual speed, while in severe sea conditions, the speed predicted by the grey-box model is slightly lower than the actual speed. However, in all sea conditions, the fuel consumption predicted by the grey-box model is very close to the actual fuel consumption, with only minor differences. The accuracy of the grey-box model meets the requirements for fuel consumption optimization. In Figures 6 and 7, the blue bars represent the actual engine fuel consumption values and actual ship speeds, the orange bars indicate the predicted fuel consumption values and

predicted ship speeds from the grey-box model, and the red dots show the absolute error between them.

Table 7. The validation results of the grey-box model.

Sea Condition Number	RPM	Speed (kn)	Fuel Consumption (kg/nm)	Simulated RPM	Simulated Speed (kn)	Simulated Fuel Consumption (kg/nm)
1	89	11	88.24	89.2	11.1	88.45
2	92	10.5	85.80	92.4	10.6	85.14
3	98	10	94.56	98.4	10.1	94.42
4	102	9	98.66	102.1	9.2	99.12
5	108	8	112.43	107.8	7.9	110.31
6	110	6	137.41	109.5	6.2	135.44

Figure 6. Actual values vs. predicted values of fuel consumption.

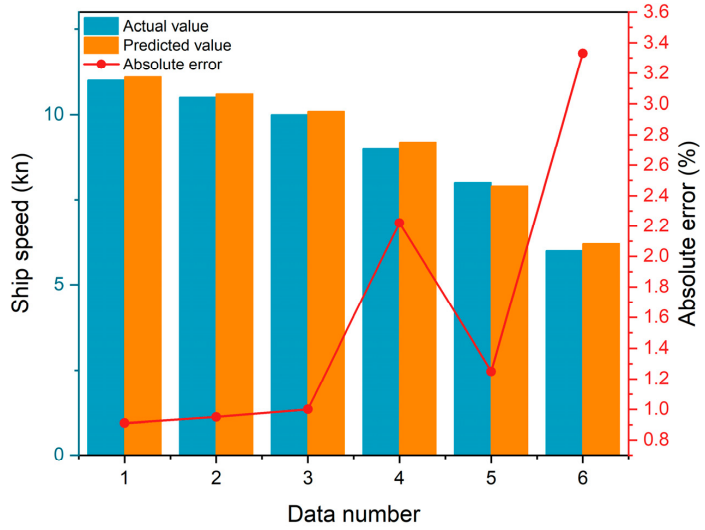

Figure 7. Actual values vs. predicted values of speed.

3. Improvement in the Non-Dominated Sorting Genetic Algorithm

The NSGA-2 algorithm [19], a commonly used multi-objective optimization algorithm, can find better solutions and convergence distributions in most problems. It is suitable

for various engineering applications, providing multiple solutions for conflicting objective functions, and has good applicability in solving speed optimization problems [17]. Based on the black-box model for fuel consumption established in the previous section, the results can form a functional relationship between the main engine speed as the optimization variable and the fuel consumption per nautical mile and speed as optimization objectives. The equation for fuel consumption per nautical mile under a specific sea condition is shown in Equation (5):

$$g_i = f_{RFR}(v_i, n_i) \tag{5}$$

where v_i is the speed under the corresponding sea condition, and n_i is the main engine's speed under the corresponding sea condition.

The optimization objective functions shown in Equations (6) and (7) can use the main engine's fuel consumption g_i and sailing speed v_i as optimization objectives during the actual navigation process, with speed n_i as the optimization variable.

$$\min f_1 = \sum_{i=1}^{n} g_i \tag{6}$$

$$\min f_2 = \sum_{i=1}^{n} v_i \tag{7}$$

The objective function for bi-objective optimization is as follows:

$$ming = min\{u_1 \cdot f_1 + u_2 \cdot f_2\}, u_1 \in [0,1], u_2 \in [0,1], u_1 + u_2 = 1 \tag{8}$$

Since there may be multiple solutions with the same non-dominance level, the initial NSGA-2 algorithm can yield multiple feasible solutions, such as solutions that favor reducing fuel consumption per nautical mile, increasing speed, or balancing both. These three types of solutions may each have multiple instances, leading to different results in each calculation, causing instability and non-uniqueness in the solutions, and making it difficult to determine the optimal speed for each sea condition. To address the shortcomings of the NSGA-2 algorithm in this study, the algorithm was optimized by constraining the main engine speed to determine the optimal speed for the main engine under various severe sea conditions. The specific optimization steps are as follows:

1. Calculate the maximum and minimum main engine speeds for the current sea condition's allowable critical safe speed under the main engine's propulsion power using the method proposed by Aertssen [28] and the minimum safe propulsion power provided by IMO [29], and then normalize these values.

$$100 \cdot \frac{\Delta v_v}{v_d} = \frac{M}{L_{pp}} + N \tag{9}$$

In Equation (9), Δv_v represents the ship's voluntarily reduced speed, v_d denotes the ship's design service speed, and 'M' and 'N' are determined by the encounter angle and wind speed, respectively.

$$P_{min} = a \cdot DWT + b \tag{10}$$

In Equation (10), DWT represents the ship's deadweight tonnage, and 'a' and 'b' are two coefficients recommended in the guidelines.

2. Apply the variable weighting method to increment u_1 and u_2 from 0 to 1 at intervals of 0.01 in the multi-objective optimization problem, using the linear weighted sum method to transform the multi-objective speed optimization problem into a single-objective speed optimization problem. Restrict the weights of u_1 and u_2 under different sea conditions: prioritize fuel consumption per nautical mile optimization ($u_1 > u_2$) for sea conditions 1 to 3 and prioritize navigation safety ($u_1 < u_2$) for sea conditions 4 to 6.
3. Discretize the main engine speed in 1 r/min increments and introduce auxiliary decision variables $h_i^j \in \{0,1\}$ according to the target requirements, further transforming

the weighted single-objective nonlinear optimization problem into a 0–1 mixed-integer linear programming problem.

4. Solve the problem multiple times under different weights to obtain the Pareto optimal solution set.
5. Use the ideal point method to balance the decisions from the obtained Pareto optimal solution set to determine a unique optimal solution and ultimately identify the best optimization speed. The ideal point principle is shown in Equation (11), where the distance of each point in the Pareto optimal solution set to the ideal point with the minimum means of the two objectives is calculated, and the point with the shortest distance is chosen as the final optimal solution.

$$minD_{opt} = min\sqrt{(f_1 - f_{1,min})^2 + (f_2 - f_{2,min})^2} \tag{11}$$

In Equation (11), D_{opt} is the distance between the Pareto frontier point and the ideal point; f_1 is the objective function value for objective 1 in the Pareto optimal solution set; $f_{1,min}$ is the minimum value of objective 1; f_2 is the objective function value for objective 2 in the Pareto optimal solution set; and $f_{2,min}$ is the minimum value of objective 2.

4. Results

The previous section introduced the steps for improving the NSGA-2 algorithm. The key to optimization lies in adjusting the objective weights u_1 and u_2 under different sea conditions, which significantly impacts the ship's speed and fuel consumption. Below, sea conditions 1 and 6 are used as examples to study the effect of different weight coefficients on the ship's speed and fuel consumption per nautical mile.

Sea condition 1 is characterized by an average wave height of 2.48 m, an average wind speed of 6.92 m/s, and a relative wind direction of 320°. For a Handymax bulk carrier, navigation under this condition is relatively safe, so more emphasis is placed on fuel consumption per nautical mile. The value of u_1 is set from 0.5 to 1 in intervals of 0.01, corresponding to a value range of 0.5 to 0 for u_2. As shown in Figure 8, the maximum allowable speed for the ship under sea condition 1 is 13.5 knots, and the minimum speed is 10 knots. The speed increases as the fuel consumption weight u_1 decreases and the speed weight u_2 increases. In Figure 8, it can be seen that fuel consumption under sea condition 1 initially increases with an increase in u_1, reaching a maximum at u_1 = 0.65, and then decreases, reaching a minimum near u_1 = 0.85. Combining Figures 8 and 9, it is evident that simply reducing the speed does not necessarily decrease the main engine's fuel consumption. The relationship between speed and fuel consumption lies between a quadratic and cubic function, closer to a cubic function, and is still consistent with the classical approximate relationship between fuel consumption and speed.

Under sea condition 6, with an average wave height of 5.3 m, an average wind speed of 13.67 m/s, and a relative wind direction of 45°, navigational safety is paramount. If head or oblique waves are encountered on the route, the relative speed between the waves and the ship is high, causing significant impact on the hull. In severe cases, this can result in large rolling motions, significant deck wetness, bottom slamming, and propeller racing. Therefore, the speed must be reasonably reduced while considering the highest possible speed to quickly exit the severe wave area. In this case, the value of u_1 ranges from 0.5 to 0, and u_2 ranges from 0.5 to 1. From Figures 10 and 11, it can be seen that under a wave height of 5 m, fuel consumption decreases with an increase in u_1, reaching a minimum at u_1 = 0.88, and then increases. However, considering both speed and fuel consumption, it can be observed that when u_1 ranges from 0.5 to 0.7, corresponding to speeds of 5.5 to 6.5 knots, the relationship between fuel consumption and speed is not the classic approximate cubic function but rather an approximate linear relationship. When u_1 ranges from 0.7 to 1, it becomes more like a quadratic function relationship.

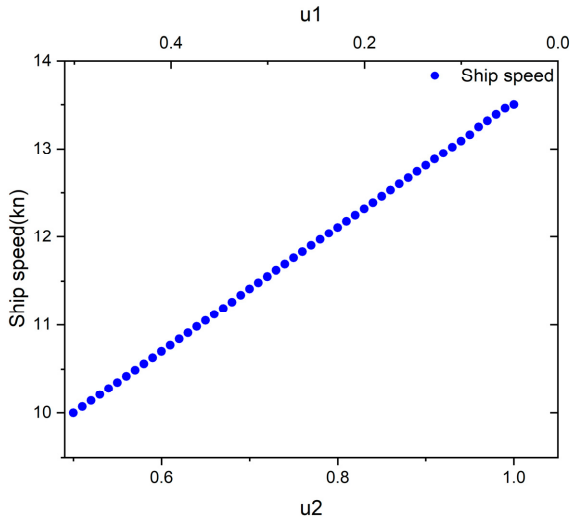

Figure 8. C1 speed weight.

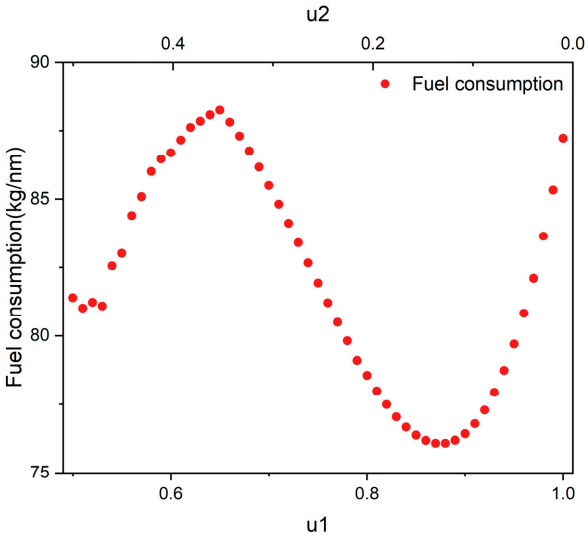

Figure 9. C1 fuel consumption weight.

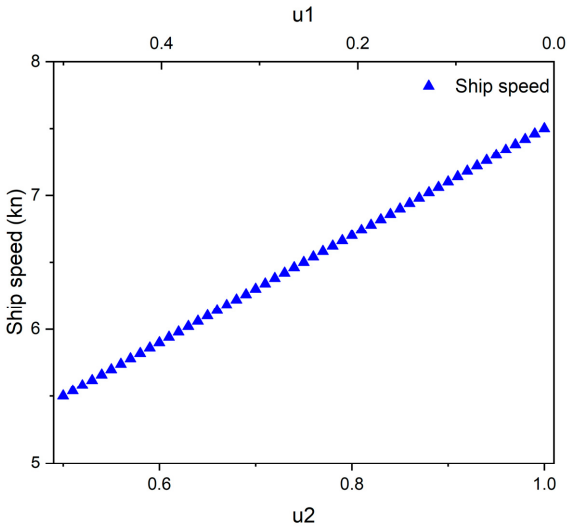

Figure 10. C6 speed weight.

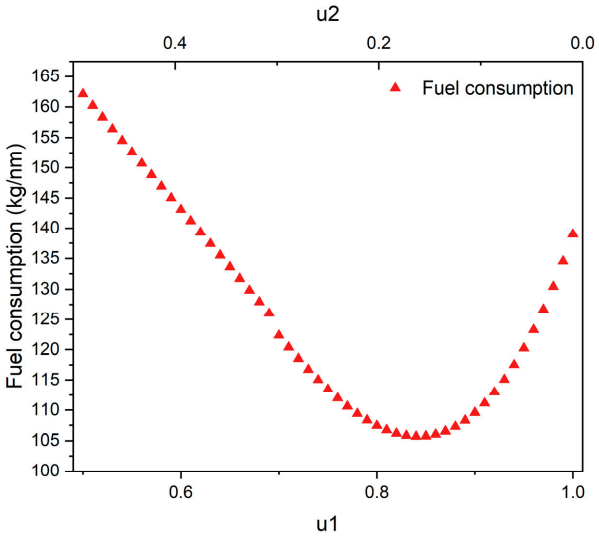

Figure 11. C6 fuel consumption weight.

By determining the optimal objective weights, u_1 and u_2, under different sea conditions, the optimal speed that balances both the navigation time and main engine's fuel consumption was found, addressing the shortcomings of the NSGA-2 algorithm. Finally, the weights u_1 and u_2 for sea conditions 1 to 6 are shown in Table 8.

Table 8. NSGA-2 optimization weights.

Sea Condition Number	u_1	u_2
1	0.85	0.15
2	0.66	0.34
3	0.58	0.42
4	0.44	0.66
5	0.26	0.74
6	0.12	0.88

5. Discussion

By comparing the pre-optimization ship and engine data in Table 9 with the post-optimization data in Table 10, the following can be observed: Firstly, from the perspective of RPM, the optimized speeds for all sea conditions are concentrated in the range of 96–114 r/m compared to the pre-optimization range of 89–110 r/m, showing a more unified and stable characteristic post-optimization. Taking sea condition 1 as an example, the engine speed before optimization was 89 rpm, which is 77% of the rated speed. After optimization, it increased to 96 rpm, which is 83% of the rated speed, enabling the engine to operate at its optimal condition for this sea state with an optimization rate of 10%. The optimal engine speeds for sea conditions 1 to 3 are 83% of the rated speed; for sea condition 4, it is 86%; and for the more severe sea conditions, 5 and 6, the optimal engine speeds are 97% and 98% of the rated speed, respectively. This concentrated and unified speed setting helps improve the operational efficiency and reliability of the main engine.

Secondly, in terms of speed, the optimized data show a significant increase in speed under most sea conditions. For example, the speed for sea condition 1 increased from 11 knots pre-optimization to 12.4 knots post-optimization, representing an improvement of 10.9%, and the speed for sea condition 2 increased from 10.5 knots to 11.8 knots, representing an improvement of 12.3%. Even under low-speed conditions (such as sea condition 6), the speed increased from 6 knots to 7 knots, representing an improvement of 16.7%. These improvements not only help reduce the navigation time but also reduce the operational costs of the ship. The most significant change is in fuel consumption, which significantly decreased under all sea conditions post-optimization. The most notable optimization is seen

in sea condition 6, where fuel consumption decreased from 137.41 kg/nm pre-optimization to 107.41 kg/nm post-optimization, representing a reduction of 21.9%. The lowest fuel consumption in sea condition 2 also decreased from 85.80 kg/nm to 74.80 kg/nm, representing a 12.8% improvement, as shown in Figure 12. This indicates that by optimizing the main engine's speed, the engine can operate at the current optimal condition, significantly improving fuel efficiency and reducing fuel consumption per nautical mile, effectively lowering operational costs and environmental pollution. Optimizing the main engine's speed to optimize the ship's speed significantly improved fuel efficiency and navigation time. The optimized data indicate that without reducing the speed, fuel consumption was significantly reduced, and the navigation time was shortened. This optimization method is of great importance for enhancing the economic efficiency and environmental performance of ships.

Table 9. Pre-optimization ship and engine data.

Sea Condition Number	RPM	Speed (kn)	Fuel Consumption (kg/nm)
1	89	11	88.24
2	92	10.5	85.80
3	98	10	94.56
4	102	9	98.66
5	108	8	112.43
6	110	6	137.41

Table 10. Post-optimization ship and engine data.

Sea Condition Number	Optimized RPM	Optimized Speed (kn)	Optimized Fuel Consumption (kg/nm)
1	96	12.4	78.56
2	96	11.8	74.80
3	96	9.6	86.48
4	100	8.6	92.42
5	112	7.5	99.49
6	114	7	107.23

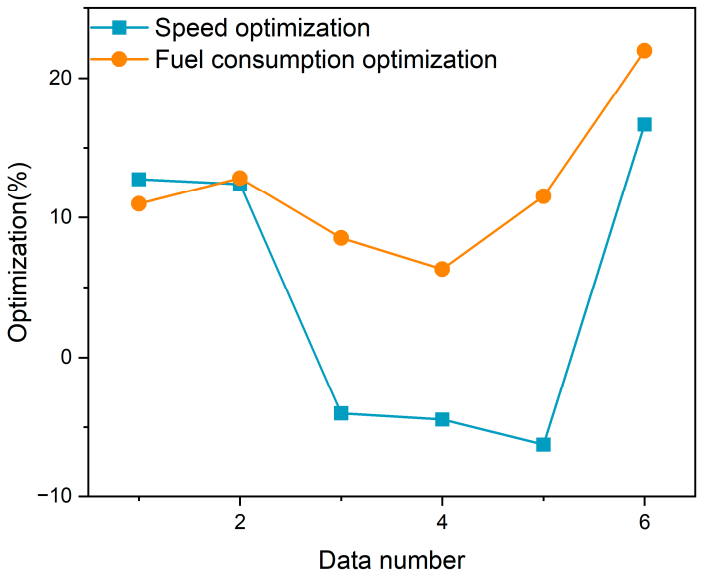

Figure 12. Speed and fuel consumption optimization.

6. Conclusions

This study investigated the impact of the main engine's speed variations on the fuel consumption of bulk carriers under severe sea conditions from the perspective of ship–engine–propeller matching using a 55,000-ton Handymax bulk carrier as the research subject. A grey-box fuel consumption model was used, with the white-box model being based on the principle of ship–engine–propeller matching. The wave-added resistance was determined using the method developed by Liu and Papanikolaou, and the wind resistance was calculated using the wind resistance coefficients provided by ITTC. The main engine parameters were determined using a combination of navigation data and bench tests, and the propeller model was determined using the regression coefficient method. Wind and wave data, as well as navigation data, were obtained from ship sensors, AIS, the ERA5 database, and ship noon reports. The K-Medoids clustering algorithm was used to classify severe sea conditions. The Random Forest Regression algorithm was used to construct the black-box energy consumption model with the main engine's speed as the variable. The fuel consumption per nautical mile and speed were the optimization objectives for the NSGA-2 algorithm. Finally, the white-box and black-box models were combined to establish the grey-box fuel consumption model. The following conclusions were drawn:

- Under severe sea conditions, reasonably adjusting the engine speed to ensure the engine operates at its optimal condition can reduce fuel consumption per nautical mile. However, excessively reducing the engine speed can lead to increased fuel consumption and decreased ship speed.
- Under severe sea conditions, increasing the main engine's speed while ensuring navigational safety and without reducing speed can significantly reduce fuel consumption per nautical mile. In sea conditions with a wave height of 5.30 m and a wind speed of 13.67 m/s, increasing the speed from 6 knots to 7 knots not only increased the speed by 16.7% but also reduced fuel consumption per nautical mile by 21.9%.
- Under severe sea conditions, the classic cubic relationship between speed and fuel consumption may not hold. In conditions with a wave height of 5.30 m and a wind speed of 13.67 m/s, the relationship between speed and fuel consumption was a combination of an approximate quadratic and linear relationship.

This study investigated the optimization of ship engine energy consumption in rough sea conditions, demonstrating the importance of adjusting the engine speed according to sea conditions. By altering the engine speed to operate at its optimal condition, the per nautical mile fuel consumption in adverse sea conditions can be significantly reduced, as well as the sailing time through these areas. Additionally, a preliminary study on the relationship between speed and fuel consumption in rough sea conditions was conducted. Future research will collect more navigation and sea condition data, further classify sea conditions, and consider the operational optimization of auxiliary engines to achieve overall energy consumption optimization for ships. Further studies will also investigate the relationship between engine fuel consumption and sea conditions in rough seas. Moreover, fuel consumption optimization for other major ship types besides bulk carriers will be conducted to ensure the model's applicability to the three main ship types.

Author Contributions: Conceptualization, Z.Y. and W.Q.; methodology, W.Q.; software, W.Q.; validation, Z.Y., W.Q. and J.Z.; formal analysis, Z.Y.; investigation, Z.Y.; resources, Z.Y.; data curation, W.Q.; writing—original draft preparation, W.Q.; writing—review and editing, Z.Y. and J.Z.; visualization, W.Q.; supervision, Z.Y. and J.Z.; project administration, Z.Y.; funding acquisition, Z.Y. and J.Z. All authors have read and agreed to the published version of the manuscript.

Funding: This research received no external funding.

Data Availability Statement: Data are contained within the article.

Conflicts of Interest: The authors declare no conflicts of interest. The funders had no role in the design of the study; in the collection, analyses, or interpretation of data; in the writing of the manuscript; or in the decision to publish the results.

References

1. IMO. *Fourth Greenhouse Gas Study 2020*; IMO: London, UK, 2020.
2. UN Trade and Development. *Review of Maritime Transport 2023*; UN Trade and Development: Geneva, Switzerland, 2023.
3. Bilgili, L.; Ölçer, A.I. IMO 2023 strategy-Where are we and what's next? *Mar. Policy* **2024**, *160*, 105953. [CrossRef]
4. Tadros, M.; Ventura, M.; Guedes Soares, C. Review of the IMO Initiatives for Ship Energy Efficiency and Their Implications. *J. Mar. Sci. Appl.* **2023**, *22*, 662–680. [CrossRef]
5. Wang, K.; Yan, X.; Yuan, Y.; Jiang, X.; Lin, X.; Negenborn, R.R. Dynamic optimization of ship energy efficiency considering time-varying environmental factors. *Transp. Res. Part D Transp. Environ.* **2018**, *62*, 685–698. [CrossRef]
6. Lee, S.-S. Analysis of the effects of EEDI and EEXI implementation on CO_2 emissions reduction in ships. *Ocean Eng.* **2024**, *295*, 116877. [CrossRef]
7. Degiuli, N.; Martić, I.; Farkas, A.; Gospić, I. The impact of slow steaming on reducing CO_2 emissions in the Mediterranean Sea. *Energy Rep.* **2021**, *7*, 8131–8141. [CrossRef]
8. Farkas, A.; Degiuli, N.; Martić, I.; Mikulić, A. Benefits of slow steaming in realistic sailing conditions along different sailing routes. *Ocean Eng.* **2023**, *275*, 114143. [CrossRef]
9. Fan, A.; Yang, J.; Yang, L.; Wu, D.; Vladimir, N. A review of ship fuel consumption models. *Ocean Eng.* **2022**, *264*, 112405. [CrossRef]
10. Tillig, F.; Ringsberg, J.W. A 4 DOF simulation model developed for fuel consumption prediction of ships at sea. *Ships Offshore Struct.* **2019**, *14*, 112–120. [CrossRef]
11. Mou, X.; Yuan, Y.; Yan, X.; Zhao, G. A prediction model of fuel consumption for inland river ships based on random forest regression. *J. Transp. Inf. Saf* **2017**, *35*, 100–105.
12. Tran, T.A. Investigate the energy efficiency operation model for bulk carriers based on Simulink/Matlab. *J. Ocean Eng. Sci.* **2019**, *4*, 211–226. [CrossRef]
13. Haranen, M.; Pakkanen, P.; Kariranta, R.; Salo, J. White, grey and black-box modelling in ship performance evaluation. In Proceedings of the 1st Hull Performence & Insight Conference (HullPIC), Turin, Italy, 13–15 April 2016; pp. 115–127.
14. Yan, R.; Wang, S.; Psaraftis, H.N. Data analytics for fuel consumption management in maritime transportation: Status and perspectives. *Transp. Res. Part E Logist. Transp. Rev.* **2021**, *155*, 102489. [CrossRef]
15. Ma, L.; Yang, P.; Gao, D.; Bao, C. A multi-objective energy efficiency optimization method of ship under different sea conditions. *Ocean Eng.* **2023**, *290*, 116337. [CrossRef]
16. Le, L.T.; Lee, G.; Kim, H.; Woo, S.-H. Voyage-based statistical fuel consumption models of ocean-going container ships in Korea. *Marit. Policy Manag.* **2020**, *47*, 304–331. [CrossRef]
17. Chen, B.; Wang, X.; Wang, R.; Qiu, X.; Zhu, Z.; Liang, M. The grey-box based modeling approach research integrating fusion mechanism and data. *J. Syst. Simul.* **2019**, *31*, 2575–2583.
18. Cai, Z.; Li, L.; Yu, L.; Li, C.; Sun, M. Diversity, quality, and quantity of real ship data on the black-box and gray-box prediction models of ship fuel consumption. *Ocean Eng.* **2024**, *291*, 116434. [CrossRef]
19. Ma, W.; Ma, D.; Ma, Y.; Zhang, J.; Wang, D. Green maritime: A routing and speed multi-objective optimization strategy. *J. Clean. Prod.* **2021**, *305*, 127179. [CrossRef]
20. Caires, S.; Yan, K. Ocean Surface Wave Time Series for the European Coast from 1976 to 2100 Derived from Climate Projections. Available online: https://cds.climate.copernicus.eu/ (accessed on 1 June 2024).
21. Deb, K.; Pratap, A.; Agarwal, S.; Meyarivan, T. A fast and elitist multiobjective genetic algorithm: NSGA-II. *IEEE Trans. Evol. Comput.* **2002**, *6*, 182–197. [CrossRef]
22. Holtrop, J.; Mennen, G. An approximate power prediction method. *Int. Shipbuild. Prog.* **1982**, *29*, 166–170. [CrossRef]
23. Liu, S.; Papanikolaou, A. Regression analysis of experimental data for added resistance in waves of arbitrary heading and development of a semi-empirical formula. *Ocean Eng.* **2020**, *206*, 107357. [CrossRef]
24. Hasselmann, K.; Barnett, T.P.; Bouws, E.; Carlson, H.; Cartwright, D.E.; Enke, K.; Ewing, J.; Gienapp, A.; Hasselmann, D.; Kruseman, P. Measurements of wind-wave growth and swell decay during the Joint North Sea Wave Project (JONSWAP). Ergaenzungsheft zur Deutschen Hydrographischen Zeitschrift, Reihe A. 1973. Available online: https://hdl.handle.net/21.11116/0000-0007-DD3C-E (accessed on 8 August 2024).
25. ITTC. *ITTC-Recommended Procedures and Guidelines, 7.5-03-02-05. Guideline on the CFD-Based Determination of Wind Resistance Coefficients*; ITTC: Zürich, Switzerland, 2021.
26. Breiman, L. Random forests. *Mach. Learn.* **2001**, *45*, 5–32. [CrossRef]
27. Butt, F.M.; Hussain, L.; Mahmood, A.; Lone, K.J. Artificial Intelligence based accurately load forecasting system to forecast short and medium-term load demands. *Math. Biosci. Eng.* **2021**, *18*, 400–425. [CrossRef]

28. Aertssen, G. Service Performance and Trials at Sea. In Proceedings of the 12th International Towing Tank Conference, Rome, Italy, 22–30 September 1969; pp. 210–214.
29. Liu, S.; Papanikolaou, A.; Shang, B. Regulating the safe navigation of energy-efficient ships: A critical review of the finalized IMO guidelines for assessing the minimum propulsion power of ships in adverse conditions. *Ocean Eng.* **2022**, *249*, 111011. [CrossRef]